

**Measurements of Confined Alphas and Tritons  
in the MHD Quiescent Core of TFTR Plasmas  
Using the Pellet Charge Exchange Diagnostic**

RECEIVED

MAY 28 1996

OSTI

S. S. Medley, R. V. Budny, D. K. Mansfield, M. H. Redi, A. L. Roquemore  
*Princeton Plasma Physics Laboratory, P. O. Box 451, Princeton, New Jersey 08543 USA*

R. K. Fisher, H. H. Duong<sup>+</sup>, J. M. McChesney, P. B. Parks  
*General Atomics, San Diego, California 92186 USA*  
<sup>+</sup> *General Atomics ORAU Fellow*

M. P. Petrov  
*A. F. Ioffe Physical-Technical Institute, St. Petersburg, 194021 Russia*

N. N. Gorelenkov  
*TRINITI, Troisk 142092 Russia*

**Abstract**

The energy distributions and radial density profiles of the fast confined trapped alpha particles in DT experiments on TFTR are being measured in the energy range 0.5 - 3.5 MeV using a Pellet Charge eXchange (PCX) diagnostic. A brief description of the measurement technique which involves active neutral particle analysis using the ablation cloud surrounding an injected impurity pellet as the neutralizer is presented. This paper focuses on alpha and triton measurements in the core of MHD quiescent TFTR discharges where the expected classical slowing down and pitch angle scattering effects are not complicated by stochastic ripple diffusion and sawtooth activity. In particular, the first measurement of the alpha slowing down distribution up to the birth energy, obtained using boron pellet injection, is presented. The measurements are compared with predictions using either the TRANSP Monte-Carlo code and/or a Fokker-Planck Post-TRANSP processor code, which assumes that the alphas and tritons are well confined and slow down classically. Both the shape of the measured alpha and triton energy distributions and their density ratios are in good agreement with the code calculations. We conclude that the PCX measurements are consistent with classical thermalization of the fusion-generated alphas and tritons.

**MASTER**

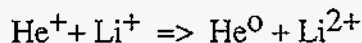
## 1.0 Introduction

The effective operation of a D-T fusion reactor requires that the alpha particles generated in D-T fusion reactions be well confined to allow deposition of most of the alpha energy in the plasma before they are lost. Based on extensive observations of fast ion behavior in tokamaks [1], alpha particles generated in D-T plasmas can be expected to thermalize classically under quiescent discharge conditions (i.e. in the absence of MHD activity and collective particle effects.) The goal of this paper is to advance the state of knowledge of alpha particles in tokamaks by presenting the first direct experimental observations showing the classical thermalization of alphas in MHD quiescent plasmas.

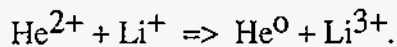
Several diagnostics designed to measure confined alphas in large tokamaks recently began operation in the tokamak experiments; namely, charge exchange spectroscopy [2] microwave scattering [3], and energetic neutral particle analysis with the use of low-Z impurity pellets [4,5]. The last method, which we call Pellet Charge Exchange (PCX), is now operated routinely on TFTR during D-T experiments. PCX diagnostic results have been reported on measurements of RF-driven energetic H,  $^3\text{He}$  and T minority ion tails [6-8], the energy distribution fast confined alpha particles [9], and the influence of magnetic field ripple and sawtooth oscillations on the behavior of the alpha energy spectra and radial density distributions [10-12]. This publication expands on work [13] presented at the 22nd EPS Conference (Bournemouth, UK, 1995).

## 2.0 Pellet Charge Exchange Diagnostic and Data Analysis

In the PCX diagnostic on TFTR, low-Z impurity pellets are injected along a midplane major radius. Upon entering the plasma, the pellet forms a toroidally elongated ablation cloud, as illustrated in Fig. 1. Using lithium pellets as an example, a small fraction of the alphas incident on the ablation cloud is neutralized either by sequential single electron capture,



or by double electron capture



If the line integral target density for particles traversing the cloud is sufficiently large, then the fraction of particles emerging from the cloud as neutrals approaches the equilibrium fraction,  $F_0^\infty(E)$ , which is independent of the linear density of the cloud. Pitch angle scattering and energy loss are not important at the pellet ablation cloud densities expected in TFTR [14].

By measuring the energy distribution,  $dn_O/dE$ , of the resultant helium neutrals escaping from the plasma, the energy distribution of the incident alpha particles,  $dn_\alpha/dE$ , can be determined using

$$dn_\alpha/dE \propto K(E) dn_O/dE \quad (1)$$

where

$$K(E) = \left\{ F_0^\infty(E) v_\alpha \frac{\Omega}{4\pi} \eta(E) \Delta E \right\}^{-1} \quad (2)$$

and

$dn_\alpha/dE$  = ion distribution in the plasma in the direction of observation,

$dn_O/dE$  = measured signal,

$F_0^\infty(E)$  = neutral equilibrium fraction,

$v_\alpha$  = ion velocity associated with energy  $E$ ,

$\frac{\Omega}{4\pi}$  = solid angle of the analyzer,

$\eta(E)$  = calibrated analyzer detection efficiency, and

$\Delta E$  = energy resolution of the analyzer.

Note that  $K(E)$  must be evaluated for the individual NPA channels. The neutral equilibrium fractions,  $F_0^\infty(E)$ , used for alphas and tritons are obtained from modeling calculations [9,14]. The NPA analyzer detection efficiency,  $\eta(E)$ , was calibrated [15] for alphas using megavolt helium ion beams generated by a cyclotron accelerator and was derived for tritons using hydrogen ions.

The escaping helium neutrals are mass and energy analyzed using a high energy (0.3 - 3.7 MeV for  $^4\text{He}$ ) neutral particle analyzer [15]. The neutral particle analyzer views the cloud surrounding the radially injected pellet from behind at a toroidal angle of  $2.75^\circ$  to the trajectory of the pellet. As a result, only near perpendicular energetic ions with velocities close to  $v_{||}/v = -0.048$  are detected by the PCX diagnostic. The radial position of the pellet as a function of time is measured using a linear photodiode array situated on the top of the vacuum vessel. By combining this measurement with the time dependence of the PCX signal, radially resolved fast ion energy

spectra and density radial profiles can be derived with a radial resolution of  $\sim 5$  cm. A more detailed description of the Pellet Charge Exchange technique and apparatus will be presented elsewhere [16].

The experimental data are compared with modeling results obtained using TRANSP [17] which is a  $1\frac{1}{2}$ -dimensional transport code (calculations of magnetic equilibrium are two-dimensional) that takes into account the spatial and temporal distributions of background plasma parameters and includes modeling of stochastic ripple diffusion of alphas [18]. Monte Carlo techniques are used to follow energetic alphas and tritons ion orbits as they thermalize and is then used to deduce the full energy and radial distribution of each species. The code assumes the alpha particles and tritons are well confined and slow down classically and includes the effects of Coulomb pitch angle scattering and velocity diffusion, but does not account for broadening of fusion-generated particles about their birth energy due to the kinetic energy of the reacting ions [19]. TRANSP provides a good calculation of the alpha and triton distributions integrated over all pitch angles. For proper simulation of the PCX measurements, however, the pitch angle should be constrained to account for only the deeply trapped particles.

TRANSP divides the pitch angle range of  $\pm 1$  into 50 equally spaced bins, giving a pitch angle resolution of 0.04. The instrumental resolution is approximately  $\pm 10^{-5}$  around the mean pitch angle value of  $v_{||}/v = -0.048$ . In order to reduce the Monte-Carlo statistical noise on the computed alpha spectra to an acceptable level, the pitch angle window in the TRANSP output cannot be constrained to less than  $-0.2 < v_{||}/v < 0.2$ , which is large compared to the narrow instrumental window. Fortunately, the alpha distribution has a weak dependence on pitch angle in this range and does not exhibit any fine grain structure. The radial averaging used in TRANSP is  $0.05r/a$  for thermal particles and  $0.1r/a$  for fast ions. For the discharges used in this paper,  $a = 80$  cm. Thus the radial averaging in TRANSP for energetic alphas and tritons is  $\sim 8$  cm compared with the instrumental value of  $\sim 5$  cm.

Although the TRANSP code is a powerful tool for analyzing experimental results, it is computationally intensive and has some severe limitations for modeling the PCX measurements. For this reason, we developed a Fokker-Planck Post-TRANSP (FPPT) processor code based on a numerical solution of the drift-averaged Fokker-Planck equation [20]. The code uses the radial and energy profiles of the pitch angle integrated alpha source from TRANSP to calculate alpha distributions for experimental conditions specific to the PCX measurements. This code includes a preliminary model for kinetic broadening of the alpha birth energy distribution, stochastic ripple diffusion effects, and sawtooth mixing of energetic particles [21]. Test calculations were made to benchmark the TRANSP and FPPT codes under conditions where stochastic ripple diffusion and MHD activity can be neglected. Good agreement was observed. The numerical FPPT code is fast and has become the standard tool for analysis of the PCX data.



### 3.0 Alpha Particle and Triton Measurements

The alpha particle distributions measured by the PCX diagnostic can be influenced by the effects of classical slowing down and pitch angle scattering, stochastic diffusion associated with toroidal magnetic field ripple, and sawtooth activity. In order to separate the classical behavior from the other effects, PCX measurements were obtained during MHD quiescent discharges in the plasma core region where stochastic ripple diffusion effects are negligible. This "plasma core" is taken to be the region well inside the boundary determined using the following expression provided by the Goldston-White-Boozer [22] theory:  $\delta_{TF} \rho q' (\pi N q / \epsilon)^{3/2} > 1$ , where  $\delta_{TF}$  is toroidal field ripple,  $\rho$  is the alpha gyro radius,  $N$  is the number of toroidal field coils,  $q$  is the safety factor,  $q' = dq/dr$ , and  $\epsilon$  is the inverse aspect ratio. The alpha slowing down spectrum for a D-T discharge (#78607) and the triton spectrum from a similar DD discharge (#78601) are shown in Fig. 2. The basic discharge parameters were:  $R_{maj} = 2.52$  m,  $a = 0.8$  m,  $P_b \sim 20$  MW with  $I_p$  ramped down from 1.7 MA to 1.0 MA during the 1.3 s duration NBI pulse. Although not specifically requested for these PCX measurements, the current ramp down scenario proved to be favorable because sawtooth-free discharges occurred at reduced neutral beam power which aided the pellet penetration. In going from alphas to tritons, the relevant values of the neutral equilibrium fraction, the ion velocity, and the analyzer detection efficiency associated with  $K(E)$  in Eq. 2 were employed using the sources given in Sec. 2. Additional plasma parameters provided by the TRANSP output immediately prior to the pellet injection time,  $t_{PCX}(s)$ , are given in Table I, where  $t_{NBI}(s)$  is the neutral beam injection period,  $S_N(s^{-1})$  is the neutron yield and  $\tau_{sl}(s)$  is the slowing down time. The midplane ripple diffusion boundaries for both 3.5 the MeV alphas and the 1.0 MeV tritons were identical to within 5% in these discharges, with a value of  $R_{rip} = 2.76$  m. The energy spectra were measured in the ripple-free region inboard of this boundary. Note that the error bars in Fig. 2 only reflect the statistical errors due to the counting statistics.

Also shown are TRANSP (solid curves) and FPPT (dashed curves) predictions of the alpha and triton energy spectra. The absolute scale for  $dn/dE$  was derived from normalization of the PCX data with the TRANSP modeling results and was made only once for the alpha data as noted in the figure. The same normalization is used for the triton spectrum. Agreement between the PCX measurements and the spectra calculated by TRANSP is quite good, indicating that the alpha and triton energy distributions and their density ratio is close to the TRANSP prediction, which assumes classical slowing down and neoclassical alpha and triton confinement. For the FPPT simulations, the shape of the energy spectra is similar, but differences occur due to the fact that Coulomb scattering is included in TRANSP but not in FPPT, which has an effect that is particularly evident toward lower energies in the slowing down distributions. For the triton spectra near the birth energy, the inclusion of a preliminary model for kinetic broadening in FPPT but not in TRANSP is the cause of the difference between the two simulations. Based on the agreement

of the energy spectra and the alpha-to-triton ratio with TRANSP predictions, we infer that fusion generated-alphas and tritons in the core of MHD quiescent TFTR plasmas are well-confined and slow down classically.

In the TFTR D-T experiments, pellets typically are injected 0.2 - 0.5 s after termination of neutral beam heating. This timing delay leads to deeper penetration of the pellet as a result of decay of the plasma electron temperature as well as to an enhanced signal-to-noise ratio because the neutron background decays significantly faster than the confined alpha population. Even so, measurements with lithium pellets result in measurable alpha signals only at alpha energies less than  $\sim 2$  MeV, as seen in Fig. 2. To enhance the pellet penetration and also to increase the signal level at higher alpha energies, we investigated the use of boron pellets in place of lithium. As seen in Fig. 3, for alpha energies above  $\sim 2$  MeV the calculated equilibrium fraction [14] for boron is significantly higher than for lithium. The higher heat of ablation energy of 5.3 eV/atom for boron compared with 1.6 eV/atom for lithium should increase the pellet penetration and consequently access a region of higher alpha density deeper in the plasma core. In practice, this gain is offset by lower pellet velocity from the injector due to the larger mass of boron relative to lithium. Nevertheless, under similar plasma discharge conditions an increase in the penetration for boron pellets ranging up to 20% ( $\sim 12$  cm) relative to lithium pellets of comparable mass is observed.

In order to validate both the use of boron and the models used for alpha neutralization in pellet clouds, alpha energy spectra were compared for D-T discharges using both lithium (#86225) and boron (# 86228, 89, 81) pellets, as shown in Fig. 4. The basic discharge parameters were:  $R_{maj} = 2.52$  m,  $a = 0.8$  m,  $I_p = 1.5$  MA and  $B_T = 5.2$  T. Additional plasma parameters are given in Table I. For this comparison, the spectra were taken near  $r/a \sim 0$  with a spatial averaging of  $\sim 10$  cm and the boron spectra for the three discharges were normalized on the basis of the D-T neutron yield to account for differences in the plasma conditions. As can be seen, the shapes of the measured alpha energy spectra for lithium and boron pellets are essentially the same, despite the very different energy dependence of the neutralization fractions used in their respective data analysis calculations. These measurements also confirm that for alpha particle energies above  $\sim 2$  MeV, boron pellets provide a more effective neutralization target than lithium pellets. The amplitude of the boron signal is approximately six times greater relative to lithium than expected on the basis of the calculated equilibrium fractions. Most likely this is due to the lithium containing a larger fraction of higher ionization states than the helium-like ionization state assumed in the analysis. Both pellet types are now routinely used in PCX diagnostic measurements.

With the capability to measure alphas up to their birth energy, alpha spectra during the birth and slowing down phases were measured using single boron pellets. Selected plasma waveforms and pellet charge exchange signals for the slowing down case (#86291,  $P_b = 15$  MW) are presented in Fig. 5. The alpha distribution from 1.0 - 3.5 MeV was obtained using a single boron pellet injected 200 ms after termination of a 1.0 s beam pulse. The basic discharge parameters

were:  $R_{\text{maj}} = 2.52$  m,  $a = 0.8$  m,  $I_p = 1.5$  MA and  $B_T = 5.2$  T. Additional plasma parameters are given in Table I. All waveforms are diagnostic measurements except for the central alpha density, which is a TRANSP calculation. Note that at the selected time of pellet injection, the D-T neutron yield which gives rise to PCX signal interference has decayed significantly while the alpha density has not. The delayed rise of the PCX alpha signal relative to the pellet light signal seen in the lower panels is characteristic of all energy channels. This behavior is attributed to stochastic ripple loss depletion effects [12] in the outboard region of the plasma which the pellet must penetrate beyond before a measurable alpha population exists at the pitch angle viewed by the PCX diagnostic.

The alpha energy spectrum obtained from the PCX measurements for this discharge using a single boron pellet is shown by the solid circles in Fig. 6. Also shown (solid squares) is the energy spectrum measured for a "beam blip" case (#86299,  $P_b = 20$  MW), where the boron pellet was injected 20 ms after a beam pulse of only 100 ms duration. The bold curves are the FPPT simulations of the PCX measurements while the lighter curves illustrate the general evolution of the alpha energy distribution at the other noted times during the 1.0 s neutral beam pulse. Reasonable agreement is seen between the data and the FPPT code results, which indicates that the alpha particles slow down classically. In addition, the absence of any peaking in the fully developed slowing down spectra in the region of 3.5 MeV indicates that massive prompt losses do not occur. This is consistent with the alpha particles being well confined. Experimental results from the  $\alpha$ -CHERS [23] and the escaping alpha [24] diagnostics on TFTR, both of which are absolutely calibrated, corroborate this classical picture of alpha behavior and also show that massive prompt losses of alphas do not occur in MHD quiescent plasma discharges.

In the "beam blip" discharge, the alphas are created in a time interval short compared to the alpha slowing-down time. In principle, the measured energy spectrum for this short pulse neutral beam injection scenario can potentially yield information on the alpha birth energy distribution. Unfortunately, the existing TRANSP code does not provide for modeling of the kinetic spreading of the alpha birth energy spectra, which must include precise information about beam energies species and injection angles, the computed thermonuclear beam-plasma and thermonuclear mix, and the ion temperature. In the FPPT code, a preliminary model of the "beam blip" data assumes simple thermonuclear Doppler broadening of the alpha particle birth energy,  $E_\alpha$ , for which the full width at half maximum is given approximately by  $\Delta E(\text{keV}) \approx 182(T_{\text{eff}})^{0.5}$  where  $T_{\text{eff}} = 30$  keV, the mean effective temperature of the deuterium and tritium ions, is based on measurement of the D-T neutron broadening in TFTR using a natural diamond spectrometer [25]. The thermonuclear formula used in FPPT is a first order approximation to illustrate the importance of the birth energy distribution for this data.

## 4.0 Discussion

The PCX diagnostic does not provide absolute alpha density measurements, which is why it is necessary to normalize the data to the TRANSP code results. While the instrumental response of the NPA analyzer was absolutely calibrated, the absolute efficiency for neutralization of the measured ions by the pellet ablation cloud is uncertain. It has been shown that provided the line integral cloud density is sufficiently high so that the charge changing reactions are independent of the density and attain an equilibrium fraction, as expected in the TFTR applications, the details of the pellet ablation cloud have little effect on the measured energy distribution but do have a strong effect on the absolute alpha density measurements [14].

The absolute magnitude of the PCX signals are well below estimates made from simple analytic calculations. A Monte-Carlo simulation of the interaction of alpha particles with pellet ablation clouds [14] which accounts for gyro orbit effects as ions traverse a pellet ablation cloud reduced the disagreement by a geometrical factor of the order of  $2\pi$ , but significant differences remain. For boron pellets, the measured signals are at least an order of magnitude lower than calculated and for lithium pellets the discrepancy is two orders of magnitude or more. We suspect that the spatial distribution of ionization states in the cloud [26] may play a key role in resolving this issue, and are configuring an array of line-filtered fiber optics to attempt measurement of this variation in the future. However, the observation that measured PCX signals are well below expectations is not yet understood.

For the discharges used in this work, the alpha population is sufficiently dilute that single-particle behavior is expected, as can be seen from the  $n_\alpha/n_e$  ratios given in Table I. To date, no 'anomalous' alpha particle losses due to alpha-driven collective instabilities have been observed in TFTR NBI-heated D-T discharges without ICRH [24,27]. This fact supports the expectation of classical ion behavior for the PCX alpha and triton measurements reported in this paper.

## 5.0 Conclusion

With the advent of D-T plasma operation on TFTR, a growing body of results from the PCX and other TFTR alpha particle diagnostics [25,26] is replacing prior speculation about alpha particle behavior. Using the PCX diagnostic, the first measurement of the alpha slowing down distribution up to the 3.5 MeV birth energy was obtained using boron pellet injection. In the core of MHD quiescent D-T discharges in TFTR, the good agreement observed between the PCX measurements of the confined, trapped alpha particles and tritons and TRANSP and FPPT



predictions is consistent with the alphas and tritons being well confined and slowing down classically.

### Acknowledgments

This work was supported by US DoE Contract DE-AC02-76-CHO-3073 and US DoE Grant DE-FG03-92ER54150.

### DISCLAIMER

This report was prepared as an account of work sponsored by an agency of the United States Government. Neither the United States Government nor any agency thereof, nor any of their employees, makes any warranty, express or implied, or assumes any legal liability or responsibility for the accuracy, completeness, or usefulness of any information, apparatus, product, or process disclosed, or represents that its use would not infringe privately owned rights. Reference herein to any specific commercial product, process, or service by trade name, trademark, manufacturer, or otherwise does not necessarily constitute or imply its endorsement, recommendation, or favoring by the United States Government or any agency thereof. The views and opinions of authors expressed herein do not necessarily state or reflect those of the United States Government or any agency thereof.

## References

- [1] Heidbrink W W and Sadler G, 1994 *Nucl. Fusion* **34** 535
- [2] McKee G et al., 1995 *Phys. Rev. Lett.* **75** 649.
- [3] Woskov P Pet al., 1988 *Rev.Sci. Instrum.* **59** 1565.
- [4] Fisher R K et al., 1988 *Fusion Technol.* **13** 536.
- [5] Fisher R K et al., 1992 *Rev. Sci. Instrum.* **63** 4499.
- [6] Medley S S et al., 1993 *Proc. 20th Euro. Conf. on Contr. Fusion and Plasma Phys., Lisbon, III* 1183.
- [7] McChesney J M et al., 1995 *Rev. Sci. Instrum.* **66** 348.
- [8] Majeski R et al., "ICRF Experiments in TFTR with Fast Waves and Mode Converted Ion Bernstein Waves," Accepted for publication in *Physics of Plasmas* (May, 1996).
- [9] Fisher R K et al., 1995 *Phys. Rev. Lett.* **75** 846.
- [10] Petrov M P et al., 1996 *Nucl. Fusion* **35** 1437.
- [11] Johnson D W et al., 1995 *Plasma Phys. Contr. Fusion* **37** A69.
- [12] Duong H H, et al., "The effects of Toroidal Field Ripple on Confined Alpha Measurements in TFTR D-T Plasmas," PPPL-3178 (March, 1996) 26 pp. Submitted to *Nucl. Fusion*. (February 1996).
- [13] Medley S S et al., 1995 *Proc. 22nd Euro. Conf. on Contr. Fusion and Plasma Phys. Bournemouth, 19C* I-409.
- [14] McChesney J M et al., 1996 General Atomics Report GA-A21958 to be submitted for publication in *Nucl. Fusion*.
- [15] Izvozchikov A B et al., 1991 Report JET-R(91) 12.
- [16] Medley S S et al., "Design and Operation of the Pellet Charge Exchange Diagnostic for Measurement of Energetic Confined Alphas and Tritons on TFTR," PPPL-3173 (April, 1996) 31 pp. Accepted for publication in *Rev. Sci. Instrum.*
- [17] Budny R V 1994 *Nucl. Fusion* **34** 1247.
- [18] Redi M H et al., accepted for publication in *Nucl. Fusion* 1995.
- [19] Sadler G J and van Belle P, 1995 *Proc. 22nd Euro. Conf. on Contr. Fusion and Plasma Phys. Bournemouth, 19C* II-269.
- [20] Gorelenkov N N and Putvinskij S V 1989 *Sov. J. Plasma Phys.* **15** 80.
- [21] Gorelenkov N N et al., "Modeling of  $\alpha$ -Particle Redistribution by Sawteeth in TFTR," PPPL-3184 (April, 1996) 17 pp. To be submitted to *Nuclear Fusion*.
- [22] Goldston R J et al., 1981 *Phys. Rev. Lett.* **47** 647.
- [23] McKee G et al., 1995 *Phys. Rev. Lett.* **75** 649.

- [24] Zweben S J *et al.*, 1995 *Nucl. Fusion* **35** 893.
- [25] Krasilnikov A V *et al.*, "TFTR Natural Diamond Detector Based D-T Neutron Spectrometry System," Submitted to *Rev. Sci. Instrum.*
- [26] Parks P B *et al.*, 1988 *Nucl. Fusion* **28** 477.
- [27] Bell M G *et al.*, 1995 *Nucl. Fusion* **35** 1429.

Table I

Selected Plasma Parameters for PCX Measurements of Tritons and Alphas.

Discharge & Type	t <sub>NBI</sub> (s)	t <sub>PCX</sub> (s)	T <sub>e</sub> (0) (keV)	n <sub>e</sub> (0) (10 <sup>19</sup> m <sup>-3</sup> )	n <sub>α</sub> /n <sub>e</sub>	Z <sub>eff</sub> (0)	S <sub>N</sub> (s <sup>-1</sup> )	τ <sub>SI</sub> (s)
78601 D-D <sup>*</sup>	2.4-3.2	3.43	6.0	2.70	1.3x10 <sup>-5</sup>	3.1	4.0x10 <sup>14</sup>	1.30
78607 D-T	2.4-3.2	3.43	4.5	2.45	2.2x10 <sup>-3</sup>	2.8	1.8x10 <sup>16</sup>	0.60
86228 D-T	3.0-4.0	4.22	7.0	2.37	4.6x10 <sup>-3</sup>	3.1	8.0x10 <sup>16</sup>	1.14
86289 D-T	3.0-4.0	4.22	5.9	2.18	5.0x10 <sup>-3</sup>	3.0	4.9x10 <sup>16</sup>	1.03
86291 D-T	3.0-4.0	4.22	5.8	2.00	4.9x10 <sup>-3</sup>	3.0	5.0x10 <sup>16</sup>	1.08
86299 D-T	3.9-4.0	4.03	6.0	3.00	7.0x10 <sup>-3</sup>	2.9	2.0x10 <sup>14</sup>	NA

\* Note that for this D-D discharge only, the table entries for n<sub>α</sub>/n<sub>e</sub> and τ<sub>SI</sub> (s) apply to tritons and S<sub>N</sub> (s<sup>-1</sup>) is the 2.5 MeV neutron rate. For the remaining discharges, entries correspond to alphas and 14 MeV neutrons in D-T plasmas.

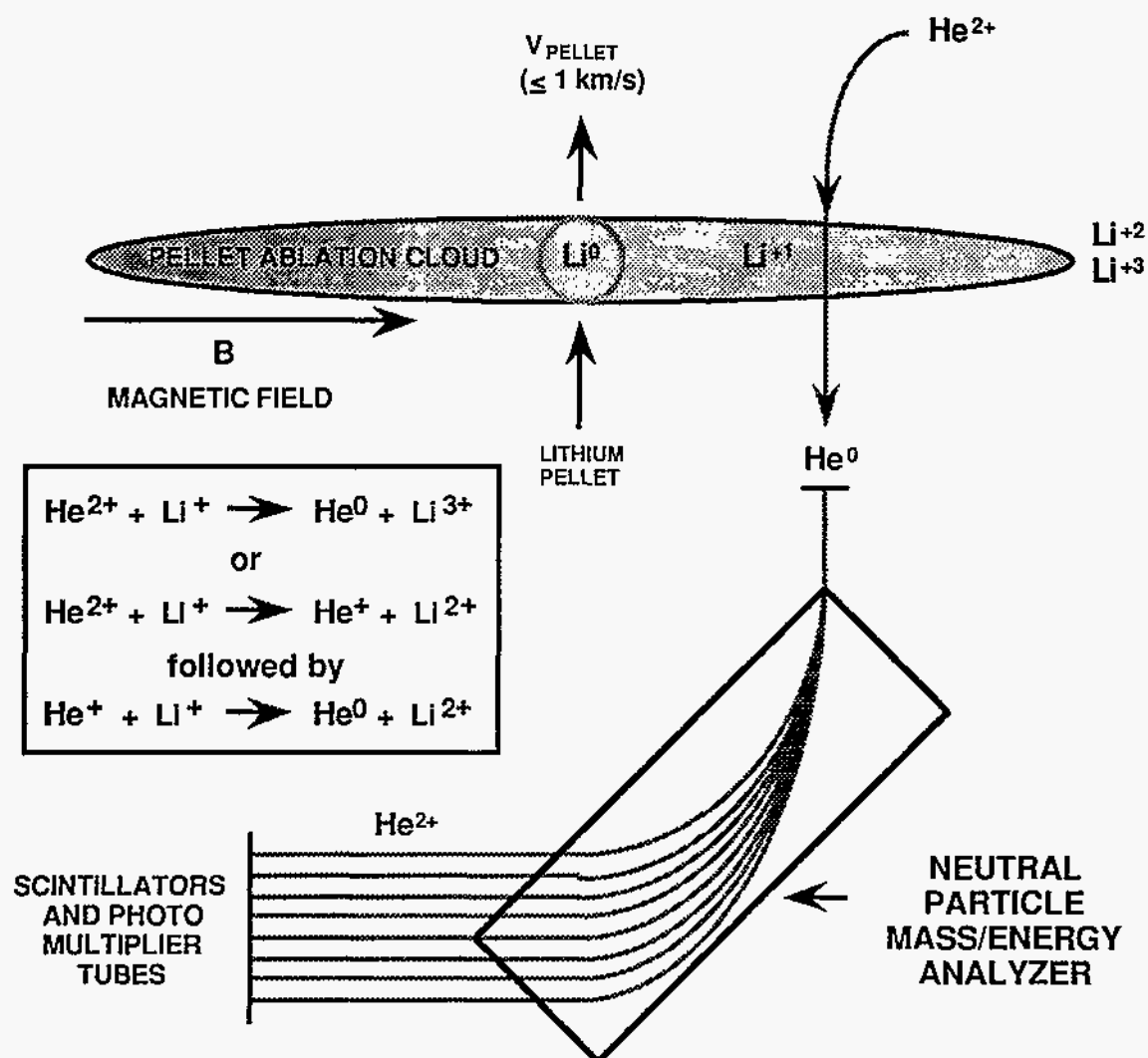


Fig. 1 Illustration of the Pellet Charge Exchange (PCX) concept using lithium as an example of low-Z impurity pellet injection.



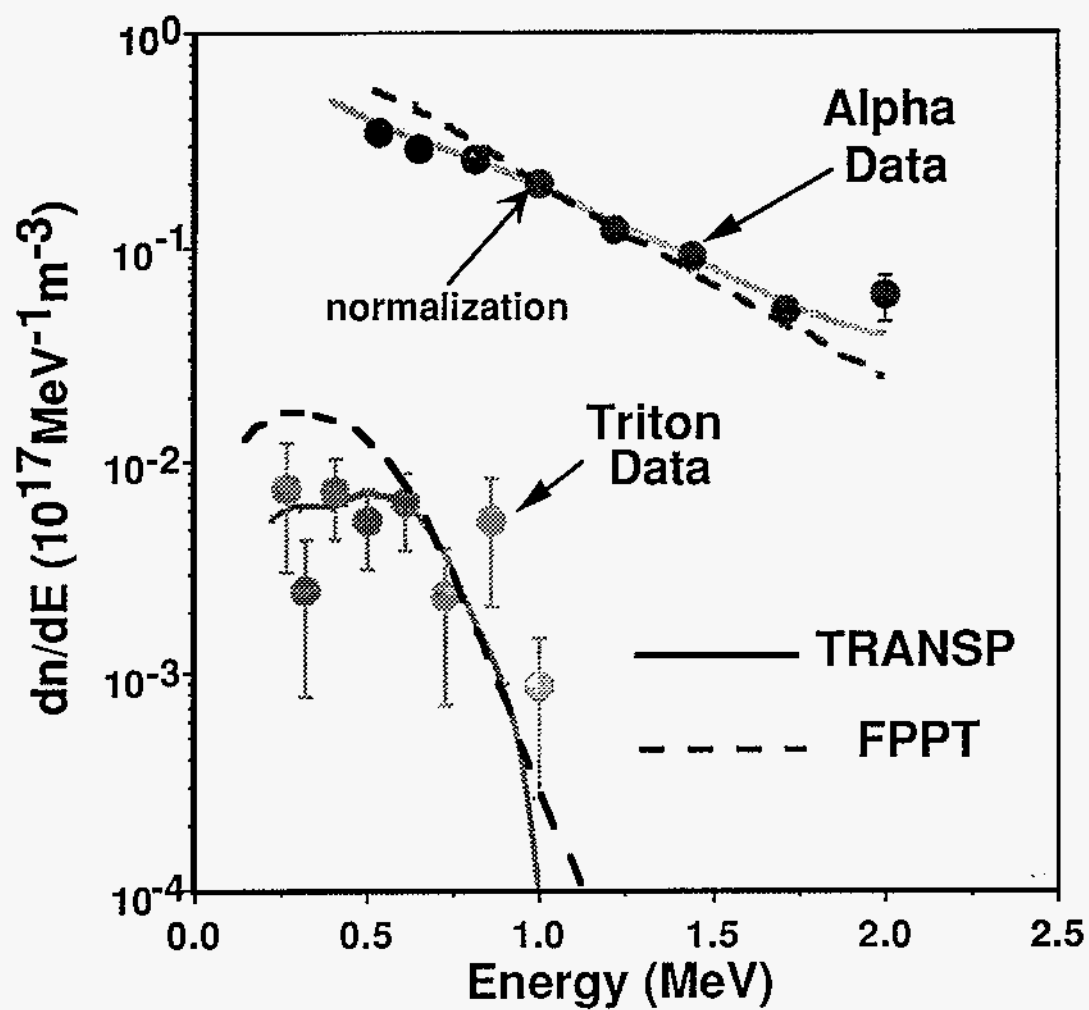


Fig. 2 Comparison of the PCX measurements of the alpha and triton spectra with TRANSP and FPPT predictions.

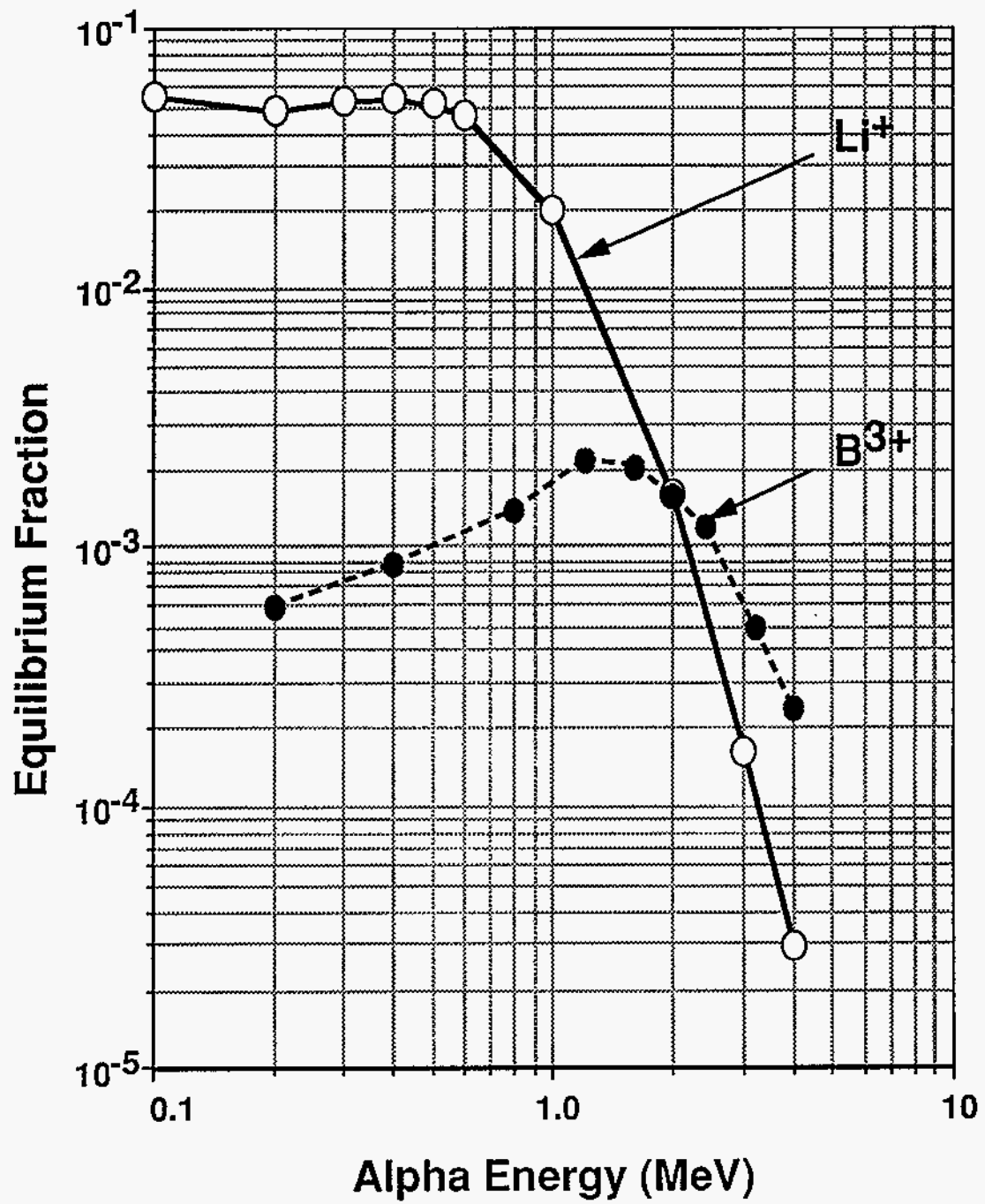


Fig. 3 Calculated neutral equilibrium fractions for alpha particles on helium-like lithium and boron.

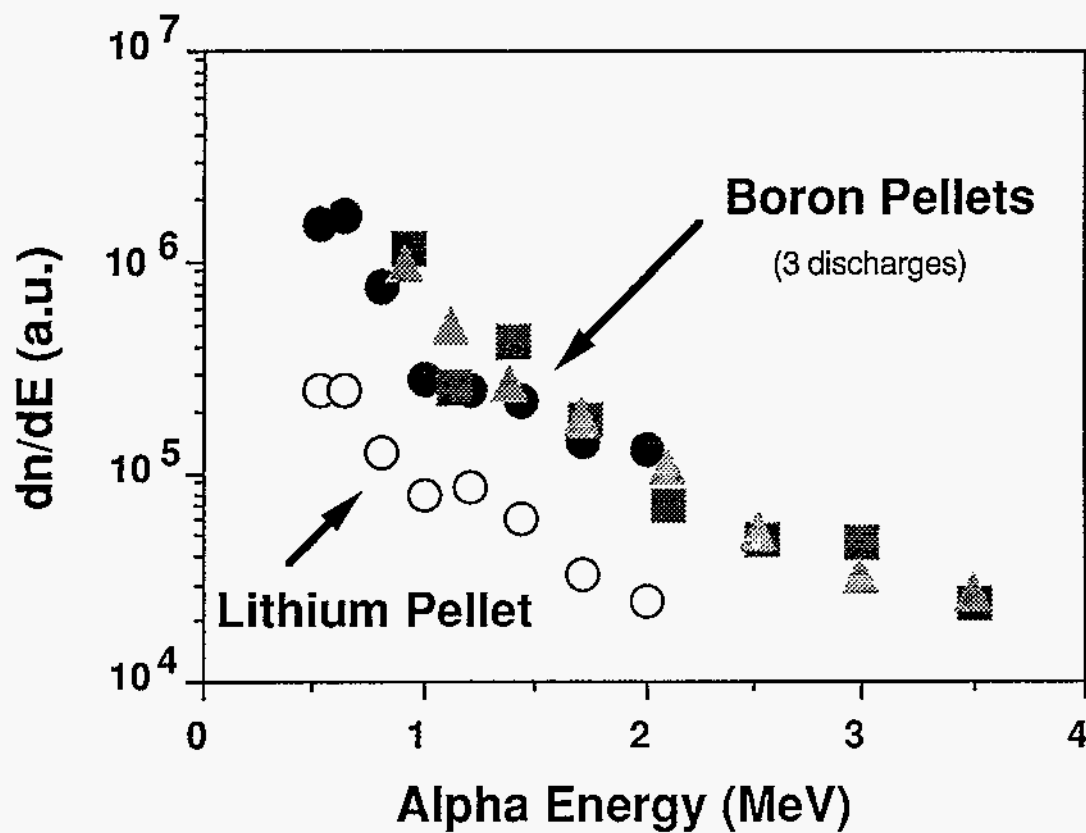


Fig. 4 Comparison of alpha spectra obtained using boron and lithium pellets.

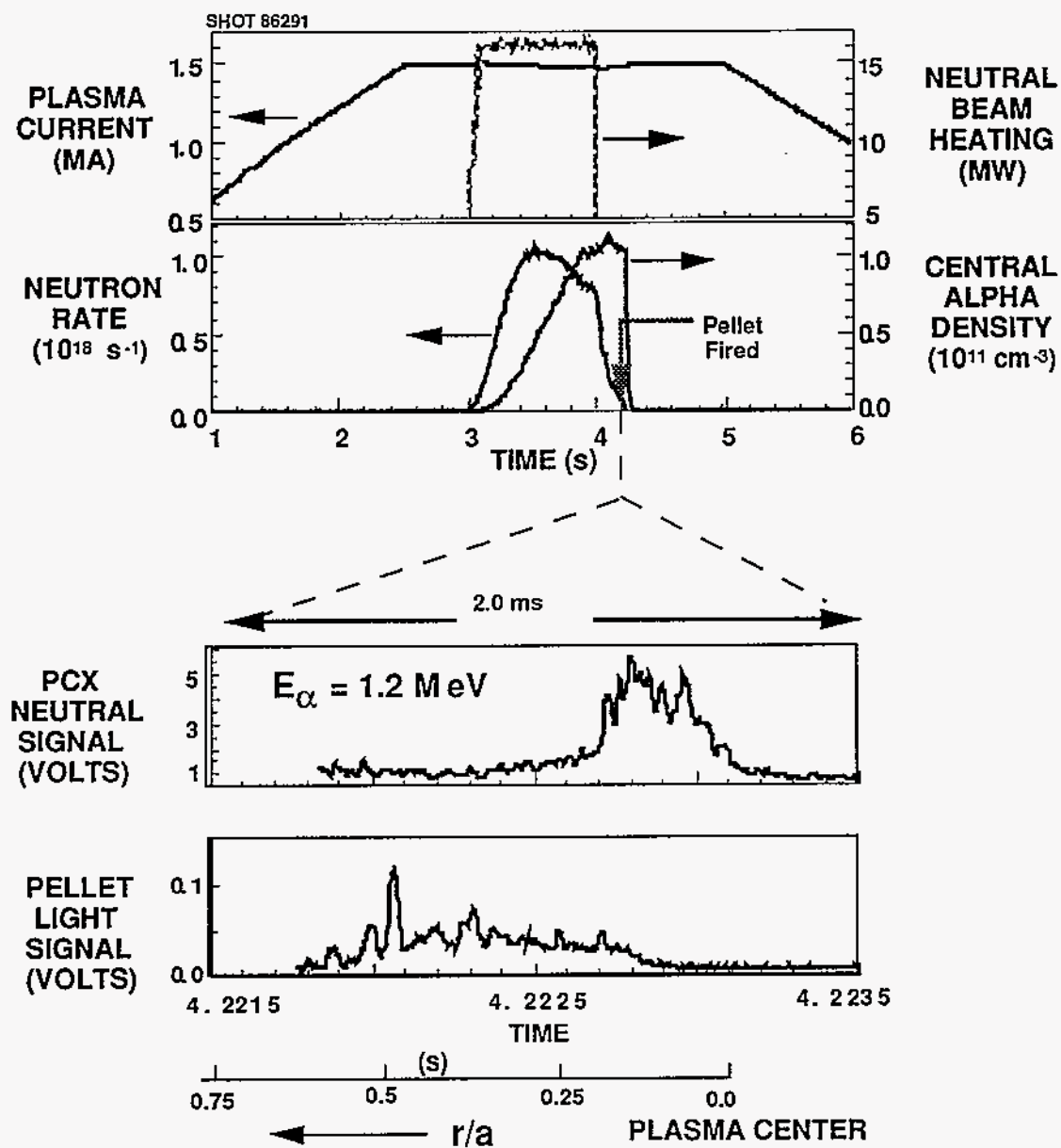


Fig. 5 Selected plasma waveforms and PCX signals for measurement of the alpha spectrum up to the birth energy using single boron pellet injection.

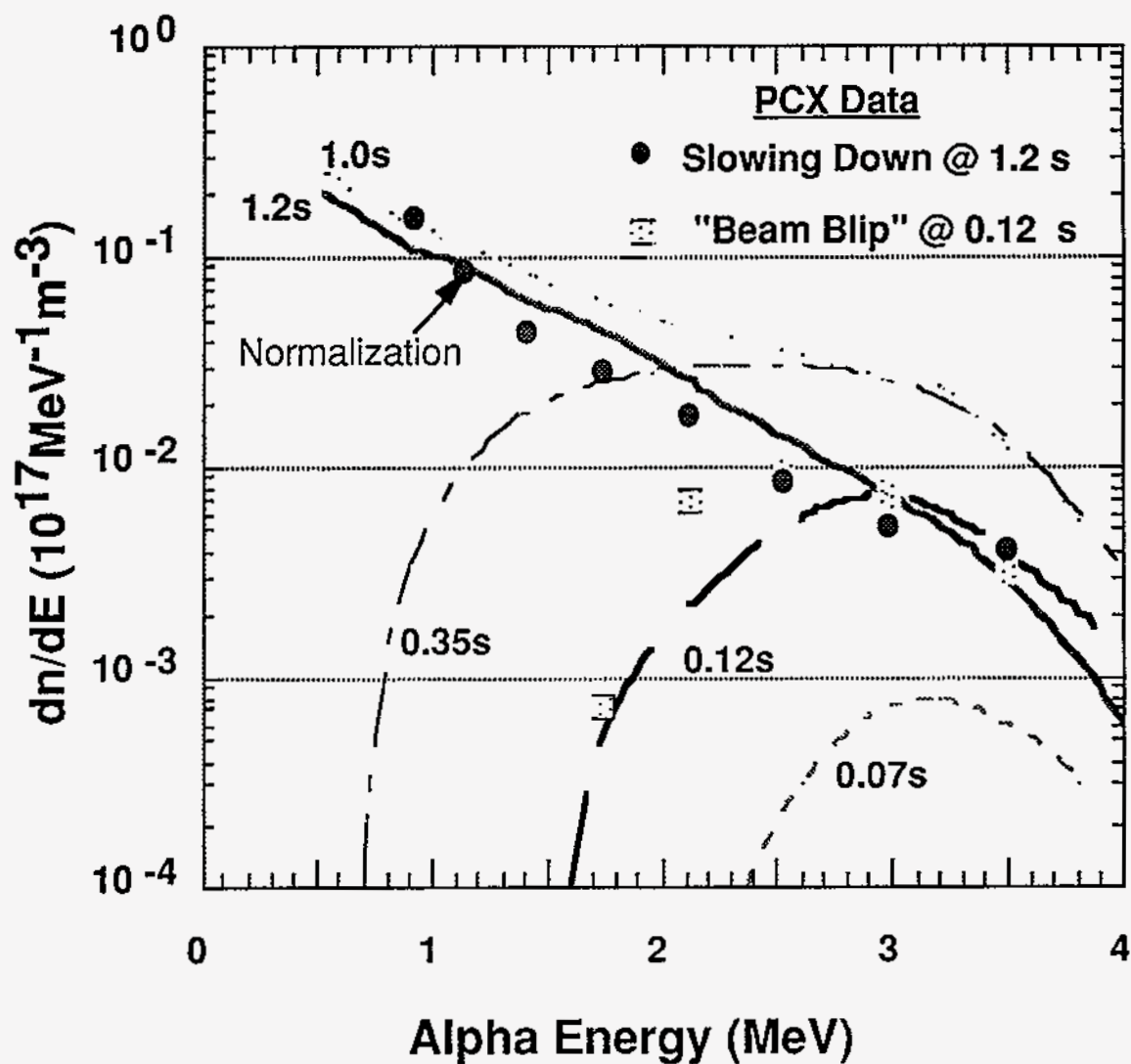


Fig. 6 Evolution of the alpha energy spectra computed using the FPPT code (curves) and comparison with the measured alpha spectra for two times: 1) during the slowing down phase shown as solid circles corresponding to 1.2 s, and 2) near the birth phase shown as solid squares corresponding to 0.12 s.



